

# Electronic Supporting Information

## The Role of Domain Size and Titanium Dopant in Nanocrystalline Hematite Thin Films for Water Photolysis

Danhua Yan,<sup>†,‡</sup> Jing Tao,<sup>¶</sup> Kim Kisslinger,<sup>†</sup> Jiajie Cen,<sup>‡</sup> Qiyuan Wu,<sup>‡</sup>

Alexander Orlov,<sup>‡</sup> and Mingzhao Liu<sup>\*,†</sup>

<sup>†</sup>*Center for Functional Nanomaterials, Brookhaven National Laboratory, Upton, New York  
11973, United States*

<sup>‡</sup>*Department of Materials Science and Engineering, Stony Brook University, Stony Brook, New  
York 11794, United States*

<sup>¶</sup>*Condensed Matter Physics and Materials Science Department, Brookhaven National  
Laboratory, Upton, New York 11973, United States*

E-mail: mzliu@bnl.gov

**Samples studied in this work and their naming (25 nm thickness of iron deposition)**

	0 atom% Ti-doping	0.5 atom% Ti-doping	1.9 atom% Ti-doping
1.0 sccm O <sub>2</sub>	Sample <b>ATi</b> <sub>0</sub>	Sample <b>ATi</b> <sub>0.5</sub>	Sample <b>ATi</b> <sub>1.9</sub>
1.5 sccm O <sub>2</sub>	/	Sample <b>BTi</b> <sub>0.5</sub>	/
2.5 sccm O <sub>2</sub>	/	Sample <b>CTi</b> <sub>0.5</sub>	/
3.5 sccm O <sub>2</sub>	/	Sample <b>DTi</b> <sub>0.5</sub>	/
10.0 sccm O <sub>2</sub>	/	Sample <b>ETi</b> <sub>0.5</sub>	/

## The dependence of PEC activity on sample thickness

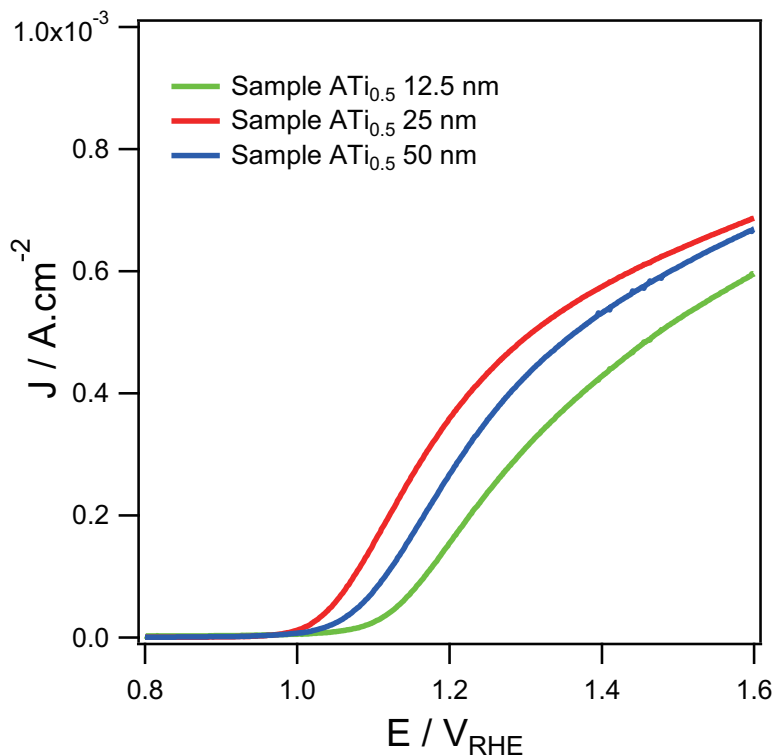


Figure S1: PEC measurements: current density vs. potential curves under AM 1.5 G illumination for hematite thin films, with same Ti-doping amount and O<sub>2</sub> flow but different thickness by QCM.

Thickness of the thin film is a crucial parameter to be considered. Figure S1 shows photocurrents of Ti-doped hematite thin films deposited under fixed O<sub>2</sub> flow (1.0 sccm) but different thicknesses in the magnetron sputtering chamber. Sample **ATi<sub>0.5</sub>** (25 nm iron) presents the highest photocurrent, with its actual thickness being around 70 nm due to the volume expansion during the RTA oxidation step. Titanium doped hematite thin film of lower or higher thickness all give smaller photocurrent. It has been believed that the PEC performance will be optimized if the electrode film thickness matches the width of depletion layer, as the carrier separation is most effective within this region.<sup>1-3</sup> Before the thickness of a thin film reaches the depletion width, thicker films will lead to an increase in photon absorption.<sup>3</sup> According to this picture, when the film thickness exceeds the depletion width, little additional photocurrent will be generated due to fast recombination process in the quasi-neutral region.<sup>4</sup> We estimate the depletion length  $d$  by treating the depletion region as

a parallel-plate capacitor, following:

$$d = \frac{\epsilon\epsilon_0 A}{C} \quad (1)$$

where  $\epsilon$  is the semiconductor dielectric constant ( $\sim 20$  for hematite),  $\epsilon_0$  the vacuum permittivity,  $A$  the surface area, and  $C$  the capacitance of the depletion region measured by the EIS method. The depletion length (at  $1.23 \text{ V}_{\text{RHE}}$ ) for Sample **ATi<sub>0.5</sub>** is found to be about 29 nm. The fact that the optimal thickness is larger than the depletion width reflects that the minority carriers (holes) may have a non-negligible diffusion length (about tens of nanometers) within the quasi neutral region.

## XPS Patterns of Ti-doped hematite thin films

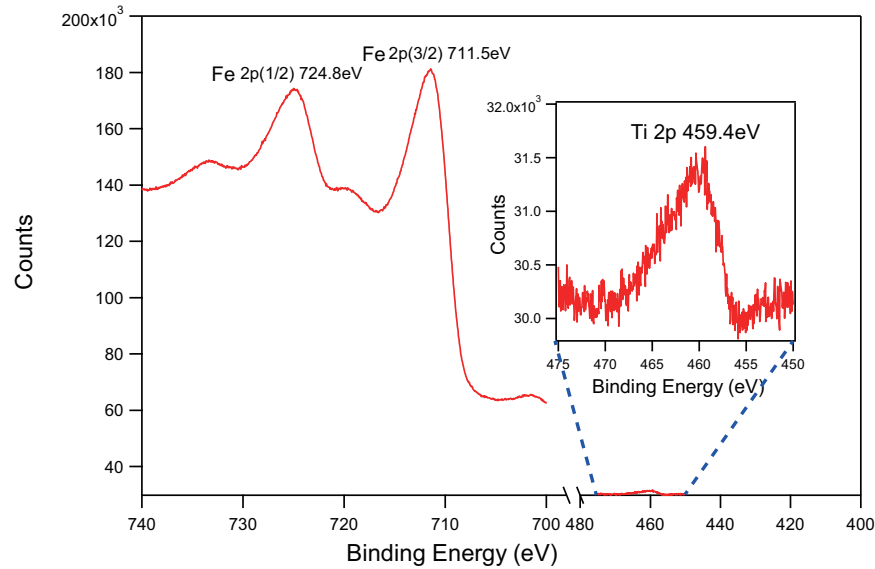


Figure S2: XPS spectrum of Sample ATi<sub>1.9</sub>, showing Fe 2*p* peaks and Ti 2*p* peak (inset). Ti 2*p* peak position indicates the valence state of titanium in hematite films to be 4+, and the doping concentration is around 2.40% according to the integrated peak area. (For XPS quantification and calibration, the sensitivity factors we adopted are from Wagner empirically database.)

X-ray photoelectron spectroscopy (XPS) finds the valence state of titanium in hematite films to be 4+ (according to Ti 2*p* peak). The titanium concentration within the sample surface could be estimated by quantitative analysis, namely by comparing the calibrated integrated peak areas of Fe 2*p* peaks and Ti 2*p* peak. In our case the dopant concentration is around 2.40 atom% for Sample ATi<sub>1.9</sub>, which confirms the result from the EDX measurement (1.90 atom%).

## Sample photos of pristine hematite thin films

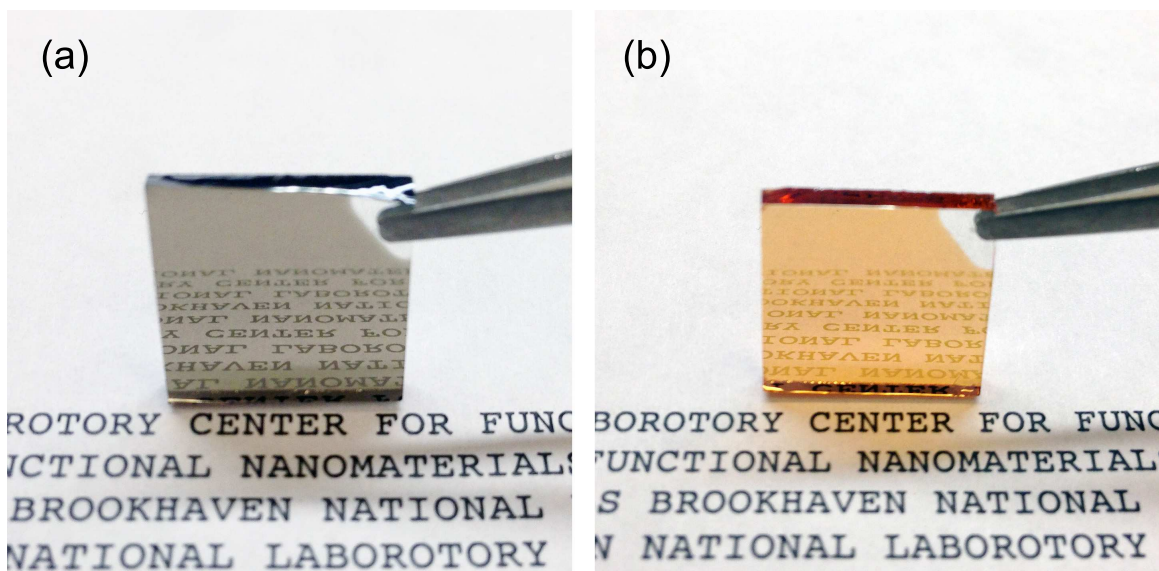


Figure S3: Samples without titanium doping: (a) as-deposit iron thin film on FTO, (b) after RTA oxidation (hematite thin film).

When deposited over FTO substrate in pure argon atmosphere, iron thin film sputtered from pure iron target features metallic smooth finish. After rapid thermal annealing (RTA) in  $O_2$ , these films are converted to uniform orange colored thin films as expected for hematite. However, Ti-doped iron thin films deposited in pure argon atmosphere appear very uneven in color after their RTA oxidation (as mentioned in the main text).

## Thermodynamic calculation of reaction between FTO and elemental titanium/iron

The chemical reaction between elemental titanium and FTO substrate follows the equation:  $\text{Ti} + \text{SnO}_2 = \text{TiO}_2 + \text{Sn}$ . Gibbs free energy ( $\Delta G$ ) is calculated to determine the reaction direction at room temperature (25°C) and at annealing temperature (500°C). The enthalpy and entropy involved are determined using thermodynamic databases\* and the Born-Haber cycle. The results are as followed:

	$\Delta H$ (kJ · mol <sup>-1</sup> )	$\Delta S$ (J · K <sup>-1</sup> · mol <sup>-1</sup> )	$\Delta G$ (kJ · mol <sup>-1</sup> )
25°C	-363.947	18.452	-369.449
500°C	-357.852	31.324	-382.069

For both circumstances we have  $\Delta G < 0$ , indicating that the reaction between Ti and SnO<sub>2</sub> is highly preferable.

On the other hand, chemical reaction between elemental iron and SnO<sub>2</sub> is not favorable during the temperature range of our experiment, according to the thermal dynamic calculations following the equation:  $4 \text{Fe} + 3 \text{SnO}_2 = 2 \text{Fe}_2\text{O}_3 + 3 \text{Sn}$ :

	$\Delta H$ (kJ · mol <sup>-1</sup> )	$\Delta S$ (J · K <sup>-1</sup> · mol <sup>-1</sup> )	$\Delta G$ (kJ · mol <sup>-1</sup> )
25°C	96.400	62.321	77.819
500°C	126.098	123.479	30.764

For both circumstances  $\Delta G > 0$ , indicating the reaction between Fe and SnO<sub>2</sub> is not likely to happen in our experimental conditions.

\*Barin I, Knacke O, and Kubaschewski O: Thermodynamic Properties of Inorganic Substances, Springer-Verlag, Berlin and New York, NY, 1973, Supplement 1977.; Barin I: Thermochemical Data of Pure Substances, VCH Verlags Gesellschaft, Weinheim, 1993.; Landolt-Brnstein: Thermodynamic Properties of Inorganic Material, Scientific Group Thermodata Europe (SGTE), Springer-Verlag, Berlin-Heidelberg, 1999.)

## XRD Patterns of Ti-doped hematite thin films on FTO glass

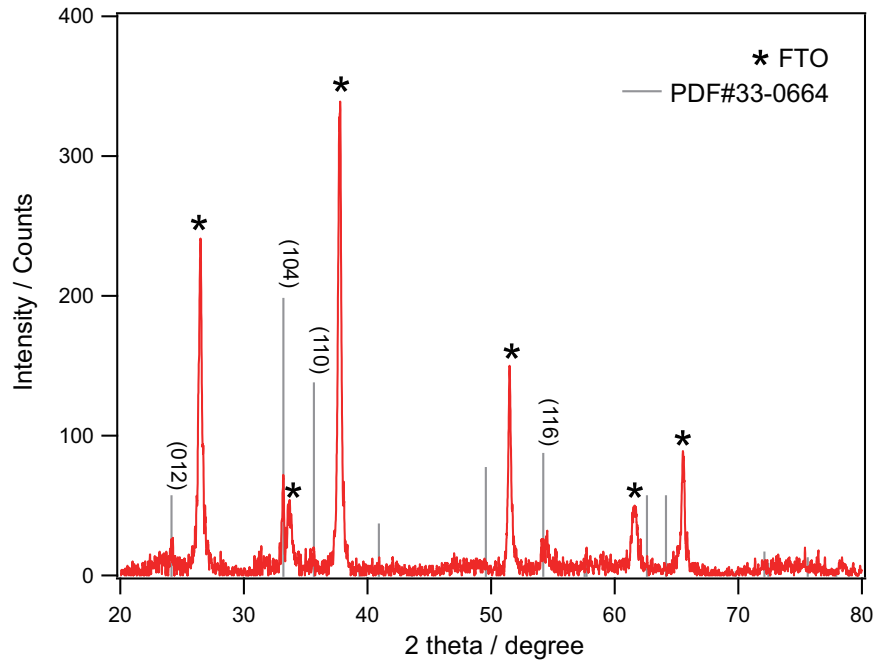


Figure S4: XRD Patterns of Ti-doped hematite thin films on FTO glass. FTO peaks marked as \*, and standard powder diffraction patterns (PDF#33-0664) of hematite are marked as grey lines.

X-ray diffraction pattern (XRD) of Ti-doped hematite thin films on FTO glasses confirms the rhombohedral lattice structures of Ti-doped hematite thin films. Diffraction peaks are indexed using a standard pattern from synthetic hematite (JCPDS#33-0664). Across all the samples we find that the strongest hematite diffraction signal is always from the (104) plane, indicating it as the preferred orientation for the hematite films, which agrees with those thin films deposited on Si wafers.



## Top-view SEM micrographs for 0.5 atom% Ti-doped hematite with different O<sub>2</sub> flow rate

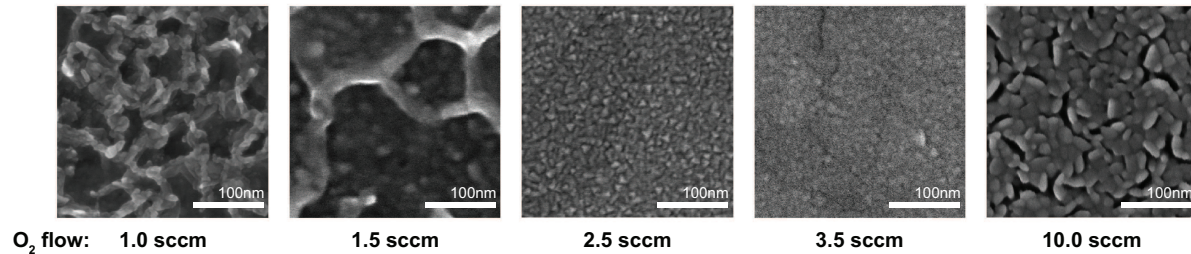


Figure S5: Top-view SEM images show the morphology and domains changes affected by different O<sub>2</sub> rate

Although Sample **ETi**<sub>0.5</sub> appears to have larger domain sizes, the appearance of gaps between each domain is worth noting. Such gaps explain the poor crystallizations and PEC performances they have, since transport of carriers become extremely difficult with such defects present.

## Current density vs. potential curves for 1.9 atom% Ti-doped films prepared with different O<sub>2</sub> flow rate

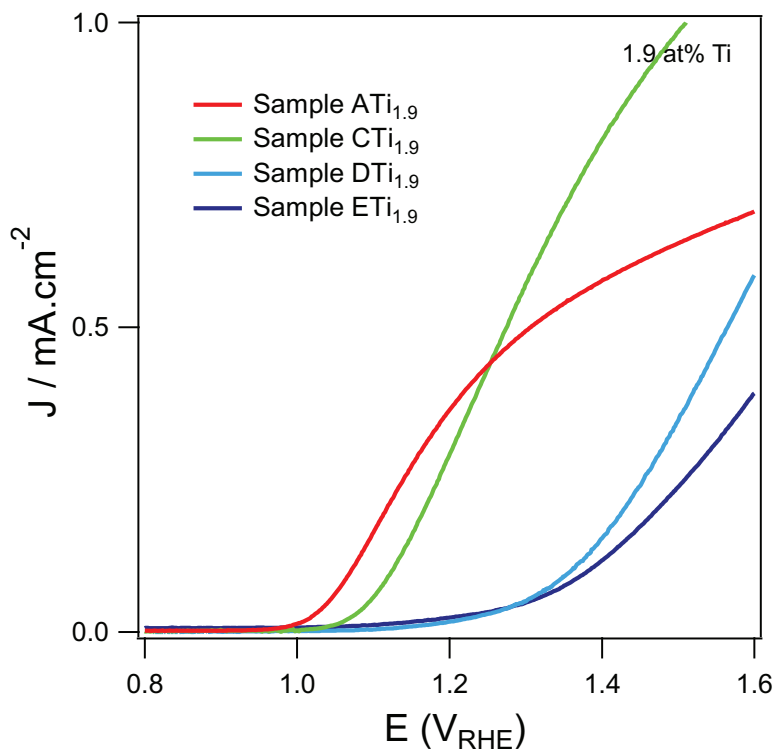


Figure S6: Current density vs. potential curves under AM 1.5 G illumination for 1.9 atom% Ti-doped films prepared with different O<sub>2</sub> flow rate during sputtering deposition.

The impact trend of oxygen flow rate on photocurrent is still true for high doping level (1.9 at% titanium doping), for the reason that the amount of oxygen is overwhelming to titanium dopants in the chamber. The drastically change in oxygen deposition atmosphere will dominate the crystallizations of hematite thin films.

## Direct and indirect band gaps of hematite determined by Tauc plots

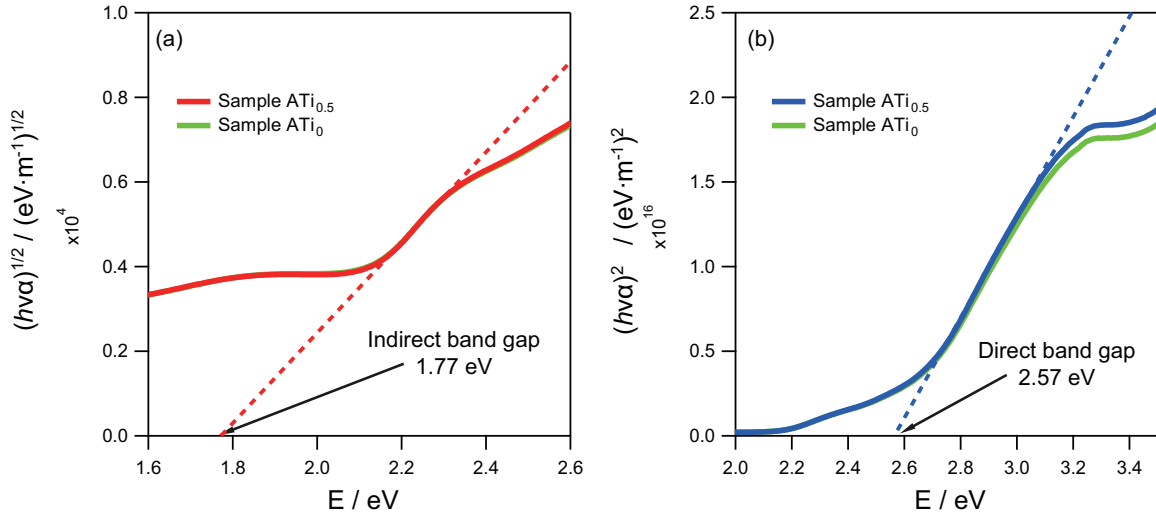


Figure S7: Direct and indirect band gap determined from Tauc Plots of Sample **ATi<sub>0</sub>** and Sample **ATi<sub>0.5</sub>**.

Tauc plot is a method that is widely used for band gap determination, which follows the relation:

$$(h\nu\alpha)^{1/n} = A(h\nu - E_g) \quad (2)$$

where  $h$  is the Planck's constant,  $\nu$  the frequency,  $\alpha$  the absorption coefficient,  $A$  the proportional constant, and  $E_g$  the band gap. For direct allowed transition, the exponent  $n$  equals  $1/2$ ; and for indirect allowed transition, the exponent  $n$  equals  $2$ . By analyzing the optical absorption spectrum of our samples we find its direct band gap at  $\sim 2.57$  eV (482 nm) and indirect band gap at  $\sim 1.77$  eV (700 nm).

## Measurement of the depletion region capacitance

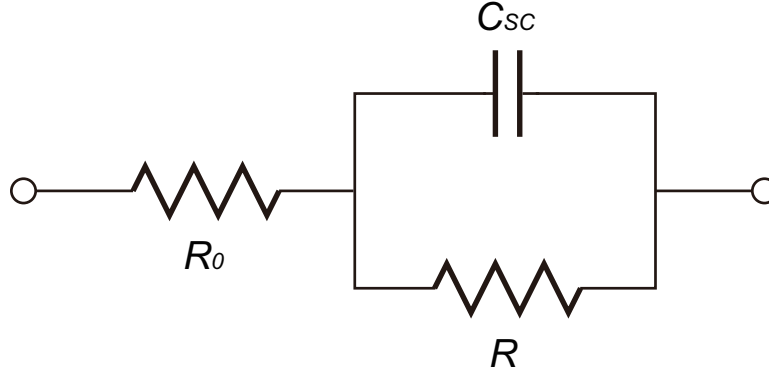


Figure S8: A conventional equivalent circuit for charge transport through depletion region.

The impedance of the PEC cell ( $Z_T$ ) is measured in the dark, at frequency  $f = 1$  kHz. Area of the working electrode  $A = 1.0$  cm<sup>2</sup>. In order to obtain barrier capacitance  $C_{SC}$  of the working electrode, the system is simplified as the equivalent circuit shown in Figure S8.

The depletion region is treated as a parallel planar capacitor, and the residue conductance due to incomplete depletion is treated as parallel resistor  $R$ . The remaining resistance in the system is regarded as a series resistor  $R_0$  to the depletion region. The impedance tested at very high frequency ( $f = 10^5$  Hz) is used as the approximation impedance of  $R_0$  ( $Z_0$ ). According to equation:

$$Z^{-1} = (Z_T - Z_0)^{-1} = R^{-1} + i\omega C_{SC} \quad (3)$$

where  $\omega$  is the angular frequency of the AC source and  $i$  is the imaginary unit, the imaginary part of  $Z^{-1}$  is related to the barrier capacitance.  $C_{SC}$  can then be calculated from:

$$C_{SC} = \text{Im}Z^{-1}/2\pi f \quad (4)$$

for each potential point for further analysis of Mott-Schottky equation.

## IPCE curves of pure hematite with an ultra-thin TiO<sub>2</sub> layer deposited by ALD

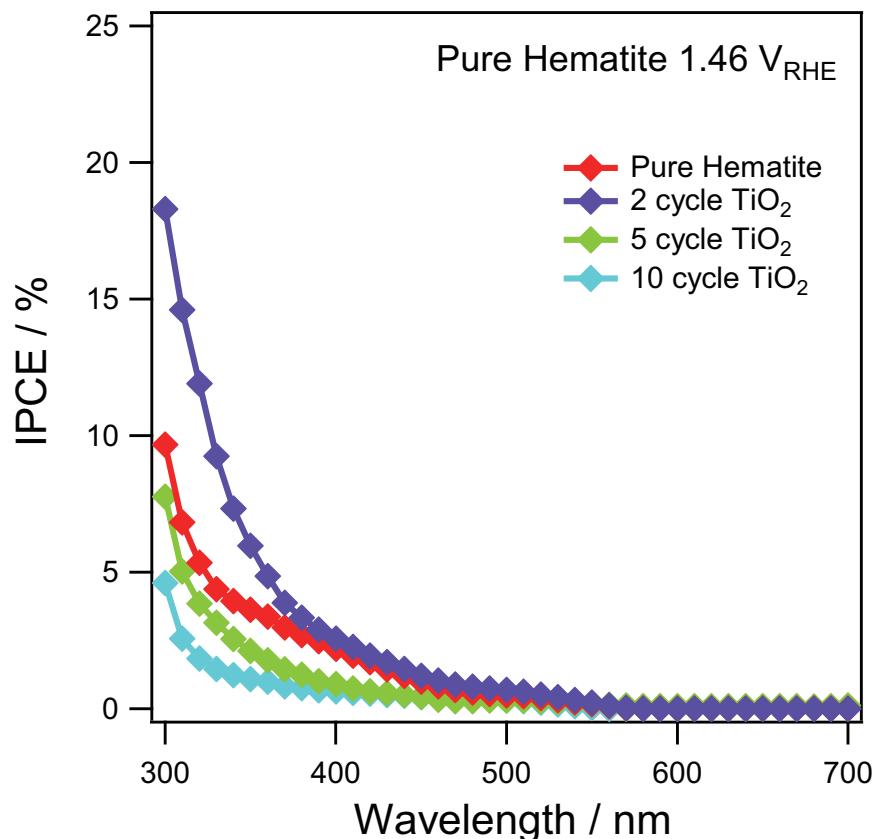


Figure S9: IPCE of pure hematite (Sample ATi<sub>0</sub>) with an ultra-thin ALD TiO<sub>2</sub> layer of various thickness, at 1.46 V<sub>RHE</sub>.

The presence of an ultra-thin layer of TiO<sub>2</sub> sub-monolayer over pure hematite thin films not only improves the overall photocurrent but also the corresponding IPCE. Only 2 cycles of TiO<sub>2</sub> (0.2 ML) could enhance the IPCE from 10% to 18% at wavelength of 300 nm.

## References

- (1) Cesar, I.; Sivula, K.; Kay, A.; Zboril, R.; Graetzel, M. *J. Phys. Chem. C* **2009**, *113*, 772–782.
- (2) Lopes, T.; Andrade, L.; Le Formal, F.; Gratzel, M.; Sivula, K.; Mendes, A. *Phys. Chem. Chem. Phys.* **2014**, *16*, 16515–16523.
- (3) Rioult, M.; Magnan, H.; Stanescu, D.; Barbier, A. *J. Phys. Chem. C* **2014**, *118*, 3007–3014.

(4) Zandi, O.; Klahr, B. M.; Hamann, T. W. *Energy Environ. Sci.* **2013**, *6*, 634–642.